Geosci. Instrum. Method. Data Syst., 6, 301–309, 2017
https://doi.org/10.5194/gi-6-301-2017

Geoscientific Instrumentation Methods and Data Systems
Open Access
EGU

Possibilities of further improvement of 1 s fluxgate variometers

Andriy Marusenkov

Lviv Centre of Institute for Space Research, Lviv, 79060, Ukraine

Correspondence to: Andriy Marusenkov (marand@isr.lviv.ua)

Received: 2 March 2017 – Discussion started: 6 March 2017
Revised: 2 July 2017 – Accepted: 13 July 2017 – Published: 23 August 2017

Abstract. The paper discusses the possibility of improving temperature and noise characteristics of fluxgate variometers. The new fluxgate sensor with a Co-based amorphous ring core is described. This sensor is capable of improving the signal-to-noise ratio at the recording short-period geomagnetic variations. Besides the sensor performance, it is very important to create the high-stability compensation field that cancels the main Earth magnetic field inside the magnetic cores. For this purpose the new digitally controlled current source with low noise level and high temperature stability is developed.

1 Introduction

Fluxgate magnetometers (FGMs) are widely used for measuring weak magnetic fields in geophysical researches. For this, reducing the FGM own noise is very important, particularly for observatory variometers compatible with the 1 s INTERMAGNET standard (Turbitt et al., 2013). The next very important task is improving the temperature stability of both the zero offset and transformation coefficient, especially for space magnetometers and geophysical equipment operating in field conditions. To achieve this, the most important thing is to improve the FGM sensor. New approaches such as the use of ferrodielectric materials (Vetoshko et al., 2003) and special excitation modes (Vetoshko et al., 2003; Koch and Rozen, 2001; Ioan et al., 2004; Sasada and Kashima, 2009; Paperno, 2004) can significantly reduce the level of own noise of fluxgate sensor, in particular, down to 0.1 pT $\mathrm{Hz}^{-0.5}$ at a frequency of 1 Hz (Koch and Rozen, 2001) with a further decrease to several tens of fT $\mathrm{Hz}^{-0.5}$ (Koch and Rozen, 2001; Koch et al., 1999). Also in the best examples of fluxgate sensors for space research, along with moderate noise level, zero offset is practically independent of temperature: their zero drift is within 1 nT in the temperature range −40 to +65 °C (Merayo et al., 2005; Nielsen et al., 1995). In this study we try to find possibilities for simultaneous improvements of noise level and temperature stability of fluxgate variometers for Earth magnetic field measurements. In Sect. 2 we describe the new fluxgate sensor with significantly reduced noise level. Then, in Sect. 3 the peculiarities of the design of a low-noise and highly stable digitally controlled current source (DCCS) are given.

2 Development of low-noise fluxgate sensor with amorphous magnetic core

During the last 10–15 years our main hopes and expectations for decreasing noise level of the fluxgate sensors have been linked with using amorphous magnetic materials instead of crystalline nickel-rich alloys (Gordon et al., 1968; Müller et al., 1998; Afanassiev, 2010, Table 3.1; Nielsen et al., 2010, pp. 154–155) for the sensor core. The very powerful technique to suppress magnetic noise of amorphous alloy is a proper annealing procedure (Shirae, 1984; Narod et al., 1985; Nielsen et al., 1991, 1995). Ten-fold improvement of the noise level is possible by selecting an optimal annealing temperature. However, we found also that the sensor's zero offset and its temperature dependence often considerably degrade after annealing. It was experimentally found that an amorphous alloy with a lower optimal annealing temperature usually could provide lower and more stable zero offset. As a result of this approach a new amorphous ring core fluxgate sensor (conventionally named FGS32/11) was recently developed. A modified version of the Co-based amorphous alloy MELTA® MM-5Co (Nosenko et al., 2008) with the Curie temperature $T_C = 185$ °C and saturation induction $B_s = 0.48$ T was used as a magnetic core. The samples of this alloy were supplied by the manufacturer in the shape of

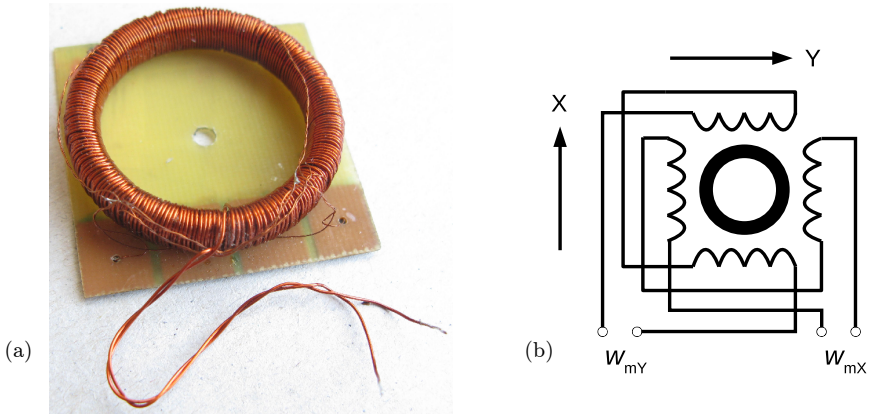

Figure 1. Fluxgate sensor FGS32/11: **(a)** general view and **(b)** measuring winding connection diagram.

0.03 mm thick and 3 mm wide tape heat treated (in the presence of a constant transverse magnetic field) at the temperature 710 K in the atmosphere of an inert gas. The 11 turns of this tape are spooled into the 32 mm diameter fiberglass bobbin that also serves as a support for the toroidally wound measuring and excitation coils (Fig. 1a). The four sectoral coils, the opposite pairs of which are connected in series, form the two measuring windings for sensing orthogonal components of the magnetic field (Fig. 1b). Such an unusual construction of the measuring windings was selected mainly because we found experimentally that (for this kind of magnetic cores) it provides a slightly better noise level in comparison with a traditional wrapping coil. The excitation winding consists of the two layers of 0.4 mm Cu wire and has little resistance, which is preferable for minimizing drive power consumption. The sensor noise level was tested with different combinations of the excitation parameters in the following ranges: the drive frequency $f_{ex} = 5$–12.5 kHz, the amplitude of the drive pulses $H_m = 2$–$10\,\mathrm{kA\,m^{-1}}$ and the relative width of these pulses $\alpha_{ex} = 0.2$–0.5. The minimal noise level was achieved with $H_m = 10\,\mathrm{kA\,m^{-1}}$ and $\alpha_{ex} = 0.5$ at the expense of considerable power consumption $P_{ex} \approx 3$ W. The compromise values $H_m = 6.8\,\mathrm{kA\,m^{-1}}$ and $\alpha_{ex} = 0.4$ were finally selected. As there was no pronounced noise level dependence on the driving frequency, the intermediate value $f_{ex} = 7.5$ kHz was selected, which gives us the possibility of driving two sensors simultaneously from a generator with a moderate output voltage $U_g = \pm 14$ V.

The zero-offset stability and the noise level measurements were conducted in a four-layer magnetic shield. The short-term zero offset drift lies within 40 pT during 7 h. The sensor noise level estimations are given in Fig. 2, where for comparison purposes a noise spectral density of the 1 s INTERMAGNET magnetometer LEMI-025 and a typical geomagnetic spectrum are presented. The achieved noise level ($\leq 1\,\mathrm{pT\,Hz^{-1}}$ at 1 Hz) is 3 times less than that of LEMI-025, which could provide better signal-to-noise ratio especially in measurements of short-period geomagnetic variations. The

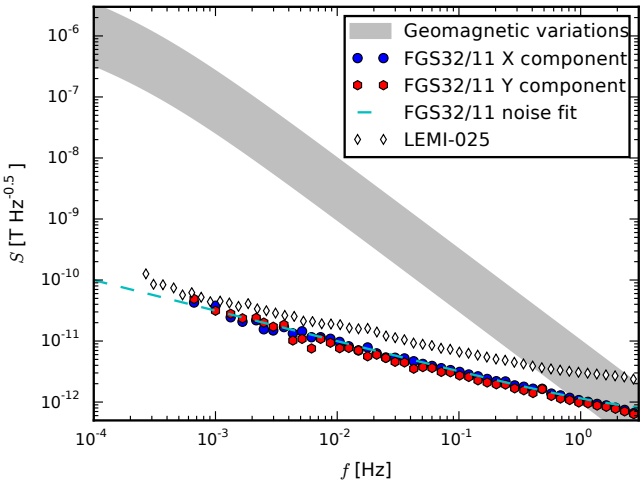

Figure 2. Noise spectra of fluxgate variometers.

zero offset drift, also measured in the magnetic chamber, does not exceed ±1 nT during sensor temperature excursions in the range +5 to +35 °C, which is comparable with the best permalloy sensors. Due to the excellent noise level, low short-term zero offset drift and good temperature stability, this sensor is very promising for use in 1 s INTERMAGNET variometers.

During our tests of the described sensor in small fields (inside the magnetic shield or installing its sensitivity axis perpendicularly to the Earth magnetic field vector) we used the sectoral measuring windings as feedback ones. However, this way is not applicable for large magnetic field measurements, because in such case the compensation field would be considerably non-uniform and, probably, unstable with temperature and time. In order to solve this problem, we are going to use these sensors as zero field indicators inside the vector compensation coil system similar to those used in spaceborne magnetometers (Auster et al., 2009; Nielsen et al., 1995). So, besides the sensor performance, it is very important to create

Table 1. Noise level of some digitally controlled current sources.

Current source	Noise level (10^{-9} Hz$^{-0.5}$)		
	0.01 Hz	0.1 Hz	1.0 Hz
Current source A (Ciofi et al., 1997)	7.5	1.4	0.27
Current source B (Scandurra et al., 2014)	No data	12	3
Current source C (Costa et al., 2012)	No data	No data	30
Requirements for the DCCS	71	22	7.1

the high-stability compensation field that cancels the main Earth magnetic field inside the magnetic cores. The possibility of constructing a DCCS with temperature and noise characteristics consistent with the parameters of the best modern fluxgate sensors is considered in the next section.

3 Development of digitally controlled current source

For the postulated goal achievement, the following noise characteristics of the compensation field were posed: noise level no more than 0.5, 1.5 and 5 pT Hz$^{-0.5}$ at frequencies of 1, 0.1 and 0.01 Hz, respectively, which constitutes 7.1, 22 and 71×10^{-9} Hz$^{-0.5}$ in relative units taking into account the compensation range of $\pm 70\,000$ nT. Instability of compensation field should not exceed 1 nT or 14 ppm in relative units in the temperature range -40 °C to $+60$ °C. As the condition of a linear dependence of compensation field on temperature, the thermal drift should be as small as ≤ 0.14 ppm °C^{-1}. The digitally controlled current source – which consists of a voltage reference (VR), a digital-to-analog converter (DAC) and voltage-to-current converter – is analyzed.

Analysis of the literature reveals that the problem of creating a stable electric current is associated with relatively high noise level of semiconductor voltage sources. Ciofi et al. (1997) showed that radical reduction of the current source noise can be achieved using a chemical voltage reference; in the paper Scandurra et al. (2014) reference voltage noise reduction was achieved using a low-pass filter that is based on supercapacitors. The current sources' noise characteristics achieved in Ciofi et al. (1997) and Scandurra et al. (2014) meet the requirements for the DCCS (Table 1). Table 1 also shows that the noise of the current source (Costa et al., 2012), which is built using semiconductor voltage reference, exceeds the specified limits several times over. Devices that developed by Ciofi et al. (1997) and Scandurra et al. (2014) are designed to work in the laboratory in a relatively narrow temperature range. The stability of these current sources under temperature, time and other factors of influence is not given, but we can assume that, for example, voltage of galvanic elements and supercapacitor parameters could significantly depend on the temperature and mechanical stress.

3.1 Voltage reference selection

Based on the detailed review of the characteristics of semiconductor integrated voltage references (Harrison, 2009), it was found that only very few models have their own noise level, temperature and time drift acceptable to be used in high-class FGMs. The low-frequency ($\leq$1 Hz) noise level characteristics of different voltage reference models are given in Table 2, which is mainly filled with data taken from Fleddermann et al. (2009) and Halloin et al. (2014). Due to a lack of experimental data on the low-frequency noise spectral density, we did not include in the table the first buried-Zener voltage reference LM199 designed by Robert Dobkin. This integrated circuit was used by Acuna et al. (1978) in the outstanding MAGSAT magnetometer, the performance characteristics of which are still impressive. An indisputable leader within all specified parameters (that was also designed by Robert Dobkin) is the buried-Zener voltage reference LTZ1000 (Harrison, 2009, p. 494) based on the subsurface Zener diode, whose positive temperature coefficient is compensated by the negative coefficient of the forward-biased base-emitter voltage of the transistor located at the same substrate. This product of Linear Technology (now part of Analog Devices) has also fairly weak dependence of the output voltage on the dose of radiation (Rax et al., 1997), which may be important for space application. Achieving a record-low temperature drift (0.05 ppm °C^{-1}) is due to controlled heating and maintaining operation temperature of the chip substrate in a very narrow range. Taking into account the significant power consumption, this way is not always acceptable in FGMs and may be unreasonable due to thermal instability of other units of the VR.

Experimental research of three samples of VR showed significant nonlinearity of the temperature dependence of the output voltage U_{REF} in the temperature compensation mode without temperature stabilization (Fig. 3), especially at the edges of the temperature range. According to Tsividis (1980) and computer modeling of the VR circuit (Fig. 4; $r_b = 0$ Ohm, R2 = 18.6 Ohm, R3 = 120 Ohm, R4 = 68.1 kOhm, R5 is absent), conducted in the LTspiceIV simulation package, nonlinearity of the temperature dependence of U_{be}(VT1) is expected. Accordingly, U_{REF} looks like a dotted curve in Fig. 3, which does not match with the measurement results

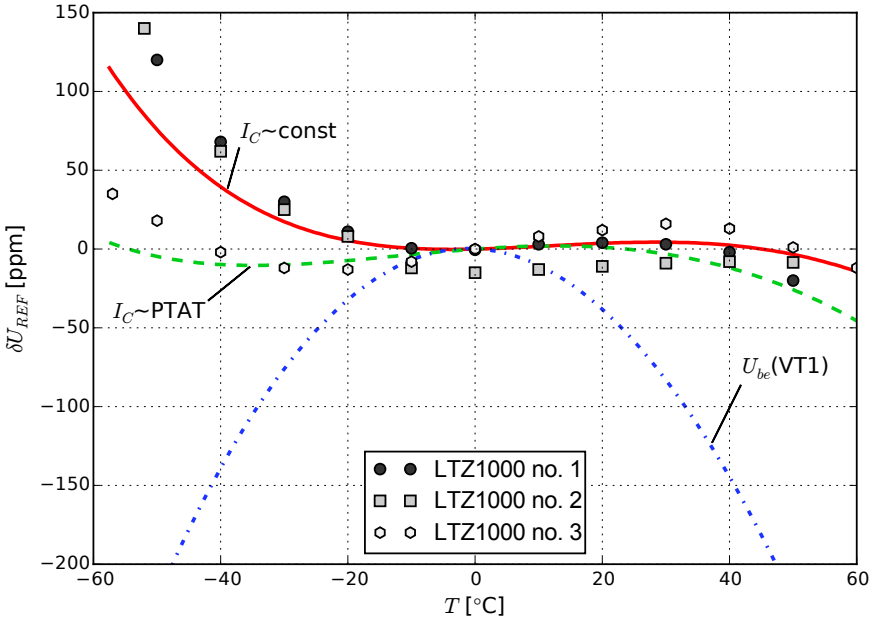

Figure 3. Temperature dependence of LTZ1000 reference voltage – simulated results (lines) and experimental data (marks).

Table 2. Noise level of some precision voltage references.

Voltage reference	Noise level (10^{-9} Hz$^{-0.5}$)		
	0.01 Hz	0.1 Hz	1.0 Hz
AD587LN (subsurface Zener) (Fleddermann et al., 2009)	250	70	19
LT1021BCN8-5 (subsurface Zener) (Fleddermann et al., 2009)	700	230	70
LT1236ACN8-5 (subsurface Zener) (Fleddermann et al., 2009)	600	130	35
LTC6655-2.5 (band gap) (Linear Technology Corp., 2014)	No data	68	28
LTZ1000 (subsurface Zener) (Linear Technology Corp., 2015)	No data	33	9
MAX6126 (proprietary) (Fleddermann et al., 2009)	230	100	50
MAX6250ACSA (subsurface Zener) (Fleddermann et al., 2009)	400	150	40
MAX6350 (subsurface Zener) (Halloin et al., 2014)	1000	600	100
VRE305 (subsurface Zener) (Halloin et al., 2014)	4000	2000	400

of output voltage of LTZ1000 samples. Much better matching of the model curve (solid line in Fig. 3) with experiment results was obtained by adding the resistor $r_b = 15$ kOhm (Fig. 4) to the LTZ1000 circuit given in the technical documentation (Linear Technology Corp., 2015).

The U_{REF} voltage increase at low temperatures is perhaps due to a decrease of the current transfer coefficient of the transistor VT1 and a corresponding increase in base current and voltage drop at r_b, R2 and dynamic resistance of the Zener diode VZ1, since a collector current depends slightly on the temperature ($\approx 0.03\,\%\,°C^{-1}$). A possible way to compensate for the effect of the temperature dependence of the base current and slightly linearize temperature dependence of U_{be}(VT1) is to generate in the VT1 collector a current I_C proportional to absolute temperature (PTAT) of the die. This method is widely used for temperature compensation in band gap voltage references (Harrison, 2009, Sect. 14.1). In contrast to band gap circuits we propose using a simpler schematic at the expense of less accurate proportionality of the current to absolute temperature. An approximately PTAT current I_C(VT1) could be generated in the diagram in Fig. 4 at a proper value of the resistor R5. The result of the simulation of the modified circuit (Fig. 4; $r_b = 15$ kOhm, R2 = 14.5 Ohm, R3 = 120 Ohm, R4 = 30.1 kOhm, R5 = 6.2 kOhm) is represented by a dashed line in Fig. 3. Experimental study of LTZ1000 sample no. 3, operating according to the modified circuit, showed that the output voltage U_{REF} temperature dependence becomes more uniform in the temperature range from 25 to 65 °C (Fig. 5). Further it is planned to get temperature characteristics of the modified circuit in a wider temperature range and specify parameters of the LTZ1000 to obtain more reliable computer simulation results.

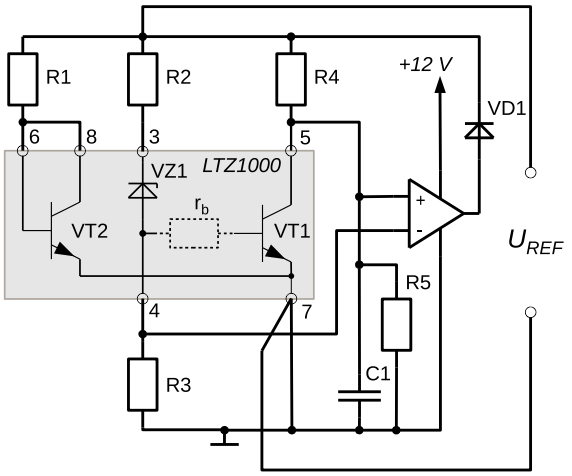

Figure 4. LTZ1000 configuration.

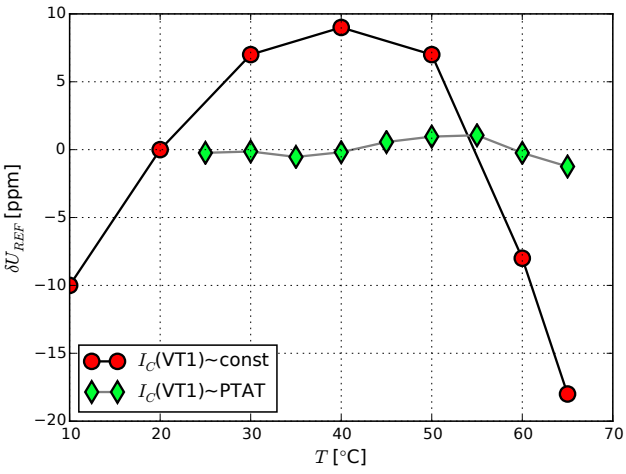

Figure 5. LTZ1000 voltage curvature correction.

3.2 DAC configuration – bipolar vs. unipolar reference input

As a digital-to-analog converter, one of the best monolithic models – a 20 bit DAC AD5791 with temperature drift 0.05 ppm °C^{-1} – was selected (Egan, 2010). As the data sheet of this component (Analog Devices, Inc., 2013) contains incomplete information regarding the noise level at low frequencies, these characteristics were examined in two circuit configurations: with bipolar (Fig. 6, circuit 1) and unipolar (Fig. 6, circuit 2) voltage reference input. The noise tests were carried out using the two samples of the DCCS: sample no. 1 with AD5791 configured for the bipolar reference input and sample no. 2 for unipolar reference input. The voltage references were built using LTZ1000. In the case of the bipolar input DAC configuration (Fig. 6, circuit 1) the negative reference output U_{REFN} was formed from the LTZ1000 positive output voltage U_{REFP} by a voltage inverter based on a low-noise operational amplifier AD8675 (Analog Devices, Inc., 2012) and a matched pair of the metal foil resistors DSMZ (Vishay Precision Group, Inc., 2015). The noise levels of both unipolar and bipolar voltage references were estimated before the DAC tests. It was found that the voltage inverter contributed practically no additional noise, so for both voltage references the noise level mainly depends on the LTZ1000 characteristics and is equal to 9×10^{-9} Hz$^{-0.5}$ at 1 Hz, 22×10^{-9} Hz$^{-0.5}$ at 0.1 Hz and 70×10^{-9} Hz$^{-0.5}$ at 0.01 Hz. In each case, the DAC output was connected to the voltage-to-current converter with an ungrounded load consisting of a low-noise zero-drift operational amplifier OPA2188 (Texas Instruments Inc., 2016) and high-stability metal foil resistors VSMP0805 (Vishay Precision Group, Inc., 2016). The noise level of these identical voltage-to-current converters was checked separately, and it did not exceed 4×10^{-9} Hz$^{-0.5}$ in the frequency band 0.01–1 Hz. For each sample, Table 3 shows the noise level of output currents at the various points in the range: at zero ("$I_{\mathrm{out}} = 0$" column), at the minimum ("$I_{\mathrm{out}} = I_{\mathrm{min}}$" column) and at the maximum values ("$I_{\mathrm{out}} = I_{\mathrm{max}}$" column). The values of the noise level which exceed given limits are marked in bold. Overpassing the requirements at a frequency of 1 Hz for both cases is caused by the voltage reference noise. The noise of the AD5791 configured with a unipolar reference input (Fig. 6, circuit 2) is considerably bigger than that of the version with a bipolar reference input and exceeds the requirements at zero and minimum values of the output current. Probably, this is due to the additional $1/f$ noise generated by the resistors R_1 and R_{FB} (see Fig. 6, circuit 2) when a larger current is flowing through them. At the bipolar input configuration (Fig. 6, circuit 1) these resistors are excluded from the signal pass and can not contribute an excessive noise. So, for achievement of better noise characteristics, the AD5791 has to be connected in the version of the bipolar voltage reference input.

3.3 The temperature stability of the DCCS

The two prototypes of the DCCS with AD5791 configured for a bipolar reference input were intensively tested in order to estimate the temperature dependences of both the separate units and the device in whole. The measurements were carried out at the five values of the DAC input code: 0x100000 ($U_{\mathrm{DAC}} = U_{\mathrm{REFN}}$), 0x13FFFF ($U_{\mathrm{DAC}} = 0.5\,U_{\mathrm{REFN}}$), 0x17FFFF ($U_{\mathrm{DAC}} = 0$ V), 0x1BFFFF ($U_{\mathrm{DAC}} = 0.5\,U_{\mathrm{REFP}}$) and 0x1FFFFF ($U_{\mathrm{DAC}} = U_{\mathrm{REFP}}$).

Let the DAC output voltage be given by the expression

$$U_{\mathrm{DAC}} = U_{\mathrm{REFP}} S_{\mathrm{DAC}} + U_{\mathrm{REFN}}(1 - S_{\mathrm{DAC}}), \quad (1)$$

where $S_{\mathrm{DAC}} = 0$–1 is the transformation factor of the DAC.

It could be shown that the relative deviation δS_{inv} of the voltage inverter scale factor S_{inv} leads to inconsistency of the positive U_{REFP} and negative U_{REFN} reference voltages and

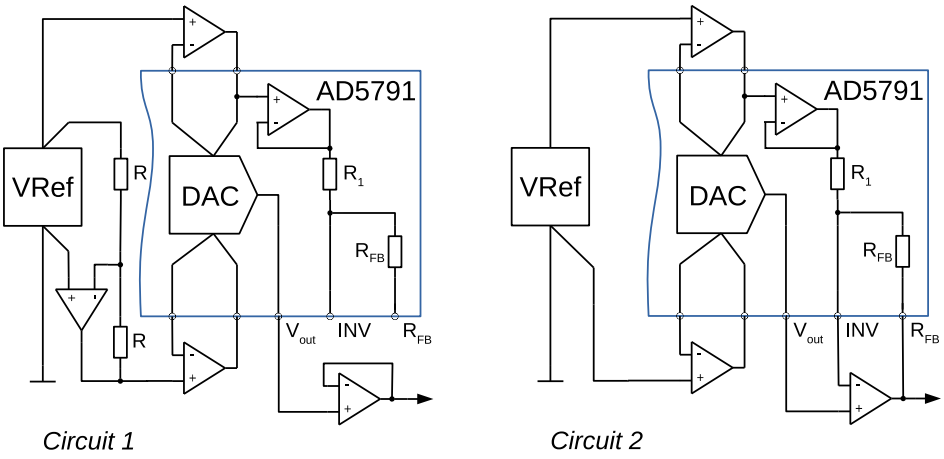

Figure 6. Digital-to-analog converter configurations.

Table 3. Noise level of the digitally controlled current source.

Frequency (Hz)	Noise level (10^{-9} Hz$^{-0.5}$)						Requirements
	$I_{out} = 0$		$I_{out} = I_{min}$		$I_{out} = I_{max}$		
	circuit 1	circuit 2	circuit 1	circuit 2	circuit 1	circuit 2	
1.0	4	**8**	**9**	**16**	**9**	**9**	≤ 7.1
0.1	7	14	22	**39**	22	22	≤ 22
0.01	15	42	70	**150**	70	70	≤ 71

causes the relative change of the DAC output voltage as follows:

$$\delta U_{\mathrm{DAC}} = \frac{\Delta U_{\mathrm{DAC}}}{U_{\mathrm{REFP}}} = -(1 - S_{\mathrm{DAC}})\delta S_{\mathrm{inv}}. \quad (2)$$

From other side the DAC output voltage could change due to the drift of the reference voltage U_{REFP} and imperfection of the internal components of the AD5791. In order to estimate full-scale and zero-scale error temperature coefficients of the AD5791, we measured simultaneously U_{REFP}, $U_{\mathrm{REFP}} + U_{\mathrm{REFN}}$ and U_{DAC} during the temperature tests and applied necessary corrections during post-processing. For instance, we estimated AD5791 zero-scale error temperature coefficient by measuring $U_{\mathrm{REFP}} + U_{\mathrm{REFN}}$ and $U_{\mathrm{DAC}}(0)$ at the nominal zero DAC output (input code 0x17FFFF, $S_{\mathrm{DAC}} = 0.5$). Then we calculated

$$\delta U_{\mathrm{DAC}} = \frac{\Delta U_{\mathrm{DAC}}}{U_{\mathrm{REFP}}}, \quad (3)$$

$$\delta S_{\mathrm{inv}} = -\frac{(U_{\mathrm{REFP}} + U_{\mathrm{REFN}})}{U_{\mathrm{REFP}}}, \quad (4)$$

and analyzing the sum $(\delta U_{\mathrm{DAC}}(0) + 0.5\delta S_{\mathrm{inv}})$ we found the zero-scale error temperature coefficient of the AD5791. The results of such measurements for DCCS no. 1 are given in Fig. 7. The total temperature drift of the DAC output voltage $\delta U_{\mathrm{DAC}}(0)$ (markers "◊" in Fig. 7) is mainly caused by instability of the voltage reference inverter (markers "□" in Fig. 7), and contribution of the AD5791 zero-scale error temperature drift (markers "○" in Fig. 7) is negligible. For both samples of the DCCS the AD5791 zero-scale error temperature coefficient did not exceed 0.03 ppm°C^{-1} in the worst case, which is approximately compatible with data sheet specifications (Analog Devices, Inc., 2013). In both prototypes the drift of the voltage inverters' scale factors S_{inv} linearly depends on temperature with coefficients 0.27 ppm °C^{-1} in prototype no. 1 and 0.45 ppm°C^{-1} in prototype no. 2. These values coincide well with the 0.5 ppm°C^{-1} maximum-temperature coefficient of the resistor ratio (Vishay Precision Group, Inc., 2015). The full-scale temperature coefficients of both AD5791s did not exceed 15 ppm in the temperature range from −40 to +60 °C.

The voltage-to-current converter transforms the DAC output voltage $U_{\mathrm{DAC}} = -7.2$ to $+7.2$ V into the output current $I_{\mathrm{out}} = -3.6$ to $+3.6$ mA. As expected, the main contribution to the temperature drift of the transformation factor S_{ui} comes from the resistor R_{ui}, which was combined from the three 680 Ohm VSMP0805 surface mount resistors connected in series. The temperature tests of the voltage-to-current converter in DCCS no. 1 are given in Fig. 8. The temperature drift of the converter zero offset (at $U_{\mathrm{DAC}} = 0$ V,

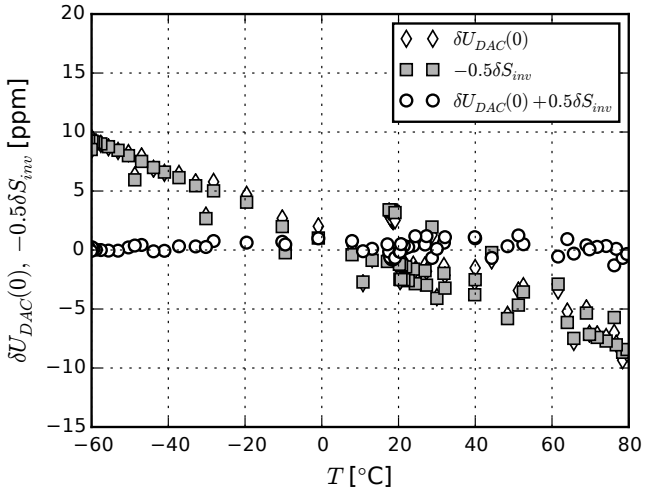

Figure 7. Temperature drift of the voltage reference inverter scale factor and the DAC zero offset.

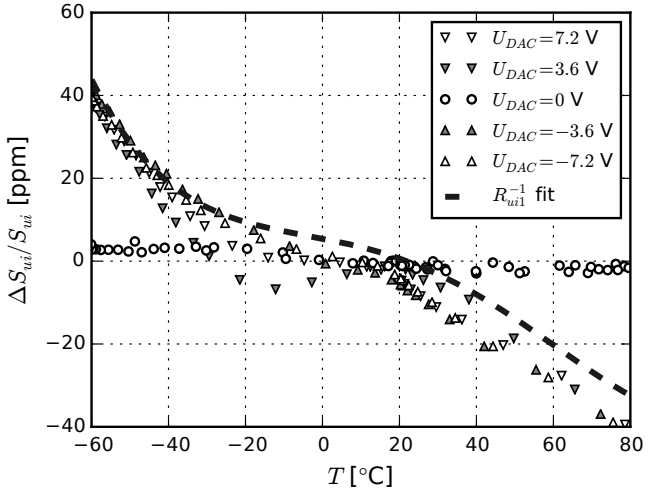

Figure 8. Temperature drift of the voltage-to-current converter transformation factor.

markers "○" in Fig. 8) does not exceed 5 ppm in the temperature range from −60 to +80 °C and is negligible in comparison with the temperature drift of the transformation factor. Similar results were obtained for the converter in DCCS no. 2, but the transformation factor temperature dependence was much more nonlinear. The temperature tests of the resistors, conducted without removing them from the boards, confirmed that R_{ui1} and R_{ui2} depend on temperature in different ways (Fig. 9), and temperature characteristics of R_{ui2} are not compatible with data sheet specifications (Vishay Precision Group, Inc., 2016). Probably, the reason for the R_{ui2} unexpected temperature dependence was that a mechanical strain occurred when the resistors were soldered on the board. The repeat temperature tests of the same resistors re-soldered in order to minimize possible package deformation reveal considerable change of the resistance temperature characteristics (see Fig. 9), which become more uniform and similar to the data sheet curve. In order to avoid the mechanical strain problems, we are going to use through-hole, hermetically sealed versions of the metal foil resistors in future designs.

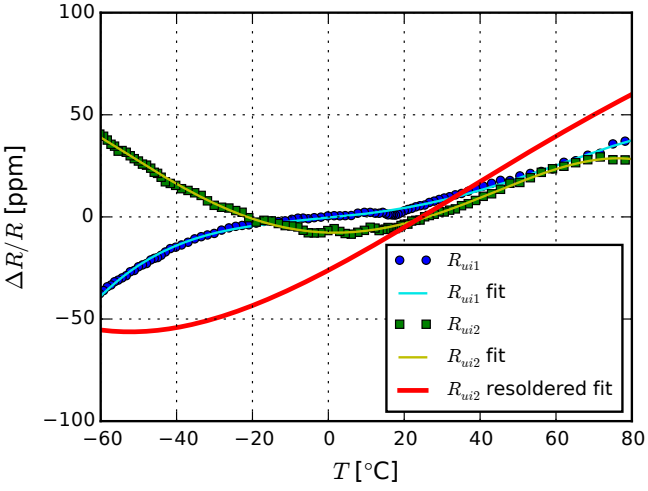

Figure 9. VSMP0805 resistors temperature dependences.

4 Conclusions

The ways to improve noise level and temperature stability of 1 s fluxgate variometers are considered. The noise parameters of the new fluxgate sensor with Co-based amorphous magnetic alloy are discussed. The achieved sensor noise level is equal to 1 pT Hz$^{-0.5}$ at 1 Hz, which is considerably better than that of the modern observatory fluxgate magnetometers. The short-term zero-offset stability of the sensor is also quite good and lies within 40 pT for 7 h. The zero-offset changes do not exceed ±1 nT during temperature excursions in the range +5 to +35 °C. Besides the sensor performance, it is very important to create the high-stability compensation field that cancels the main Earth magnetic field inside the magnetic cores. The voltage reference in the electronic unit and the compensation windings in the sensor are the most critical elements in terms of generating the stable compensation signals. The noise level, the temperature drift and the long-term stability of the best semiconductor voltage references are compared, and it is stated that only few of them are suitable for application in high-class fluxgate variometers. Using the best available electronic components, the prototypes of the digitally controlled highly stable current source are designed and tested. As a part of this work it is experimentally shown that one of the best voltage references (LTZ1000) exhibits considerable non-uniformity of the temperature dependence in the uncontrolled temperature mode. Curvature-compensating circuitry is proposed. The source of the extra noise in the digital-to-analog converter AD5791 is revealed,

and the appropriate configuration of its inner structure is selected. It is supposed that the application of the results and recommendations discussed in the paper will allow creating an FGM with outstanding level of noise and temperature parameters.

Data availability. The experimental data are not available because they have only intermediate importance and were not registered.

Competing interests. The author declares that he has no conflict of interest.

Special issue statement. This article is part of the special issue "The Earth's magnetic field: measurements, data, and applications from ground observations (ANGEO/GI inter-journal SI)". It is a result of the XVIIth IAGA Workshop on Geomagnetic Observatory Instruments, Data Acquisition and Processing, Dourbes, Belgium, 4–10 September 2016.

Acknowledgements. This work was supported by a grant of the National Academy of Science of Ukraine. The author would like to thank the Local Organizing Committee of the XVIIth IAGA Workshop on Geomagnetic Observatory Instruments, Data Acquisition and Processing for financial support.

Edited by: Arnaud Chulliat
Reviewed by: two anonymous referees

References

Acuna, M. H., Scearce, C. S., Seek, J., and Scheifele, J.: The MAGSAT vector magnetometer: A precision fluxgate magnetometer for the measurement of the geomagnetic field, Technical Memorandum NASA-TM-79656, National Aeronautics and Space Administration, Goddard Space Flight Center, Greenbelt, Maryland, available at: https://ia800302.us.archive.org/34/items/nasa_techdoc_19790010349/19790010349.pdf (last access: 2 July 2017), 1978.

Afanassiev, Y.: Magnetic Offset and Noise, in: Fluxgate Magnetometers for Space Research, edited by: Musmann, G., chap. 3, 73–112, 2010.

Analog Devices, Inc.: 36 V Precision, 2.8 nV/$\sqrt{\text{Hz}}$ Rail-to-Rail Output Op Amp. Rev. E., available at: http://www.analog.com/media/en/technical-documentation/data-sheets/AD8675.pdf (last access: 2 July 2017), 2012.

Analog Devices, Inc.: 1 ppm 20-Bit, ±1 LSB INL, Voltage Output DAC AD5791. Rev. D., available at: http://www.analog.com/media/en/technical-documentation/data-sheets/AD5791.pdf (last access: 2 July 2017), 2013.

Auster, H. U., Glassmeier, K. H., Magnes, W., Aydogar, O., Baumjohann, W., Constantinescu, D., Fischer, D., Fornacon, K. H., Georgescu, E., Harvey, P., Hillenmaier, O., Kroth, R., Ludlam, M., Narita, Y., Nakamura, R., Okrafka, K., Plaschke, F., Richter, I., Schwarzl, H., Stoll, B., Valavanoglou, A., and Wiedemann, M.: The THEMIS fluxgate magnetometer, in: The THEMIS Mission, 235–264, Springer, 2009.

Ciofi, C., Gianatti, R., Dattilo, V., and Neri, B.: Ultra Low Noise Current Sources, in: IEEE Instrumentation and Measurement Technology Conference, Ottawa, Canada, 1997.

Costa, T., Piedade, M. S., and Santos, M.: An ultra-low noise current source for magnetoresistive biosensors biasing, in: 2012 IEEE Biomedical Circuits and Systems Conference (BioCAS), 73–76, https://doi.org/10.1109/BioCAS.2012.6418507, 2012.

Egan, M.: The 20-bit DAC is the easiest part of a 1-ppm-accurate precision voltage source, Analog Dialogue, 44, available at: http://www.analog.com/media/en/analog-dialogue/volume-44/number-2/articles/20-bit-dac-and-accurate-precision-voltage-source.pdf (last access: 2 July 2017), 2010.

Fleddermann, R., Trobs, M., Steier, F., Heinzel, G., and Danzmann, K.: Intrinsic Noise and Temperature Coefficients of Selected Voltage References, IEEE T. Instrum. Meas., 58, 2002–2007, https://doi.org/10.1109/TIM.2008.2006133, 2009.

Gordon, D., Lundsten, R., Chiarodo, R., and Helms, H.: A fluxgate sensor of high stability for low field magnetometry, IEEE T. Magn., 4, 397–401, https://doi.org/10.1109/TMAG.1968.1066332, 1968.

Halloin, H., Prat, P., and Brossard, J.: Long term characterisation of electronic components, The 10th International LISA Symposium, Gainesville, Florida, USA, 18–23 May 2014, available at: http://www.phys.ufl.edu/lisasymposiumx/resources/contributions/posters/Halloin.pdf (last access: 2 July 2017), 2014.

Harrison, L. T.: Current sources & voltage references, Embedded technology series, Newnes, Amsterdam, digitaler nachdr. edn., 2009.

Ioan, C., Tibu, M., and Chiriac, H.: Magnetic noise measurement for vacquier type fluxgate sensor with double excitation, J. Optoelectron. Adv. M., 6, 705–708, 2004.

Koch, R. H. and Rozen, J. R.: Low-noise flux-gate magnetic-field sensors using ring- and rod-core geometries, Appl. Phys. Lett., 78, 1897–1899, https://doi.org/10.1063/1.1358852, 2001.

Koch, R. H., Deak, J. G., and Grinstein, G.: Fundamental limits to magnetic-field sensitivity of flux-gate magnetic-field sensors, Appl. Phys. Lett., 75, 3862–3864, https://doi.org/10.1063/1.125481, 1999.

Linear Technology Corp.: LTC6655 0.25 ppm Noise, Low Drift Precision References. Rev. E., available at: http://cds.linear.com/docs/en/datasheet/6655ff.pdf (Rev. F., last access: 17 August 2017), 2014.

Linear Technology Corp.: LTZ1000/LTZ1000A Ultra Precision Reference. Rev. E., available at: http://cds.linear.com/docs/en/datasheet/1000afe.pdf (last access: 2 July 2017), 2015.

Merayo, J. M., Brauer, P., and Primdahl, F.: Triaxial fluxgate gradiometer of high stability and linearity, Sensor. Actuat. A-Phys., 120, 71–77, https://doi.org/10.1016/j.sna.2004.11.014, 2005.

Müller, M., Lederer, T., Fornacon, K. H., and Schäfer, R.: Grain structure, coercivity and high-frequency noise in soft magnetic Fe–81Ni–6Mo alloys, J. Magn. Magn. Mater., 177, 231–232, https://doi.org/10.1016/S0304-8853(97)00672-0, 1998.

Narod, B. B., Bennest, J. R., Strom-Olsen, J. O., Nezil, F., and Dunlap, R. A.: An evaluation of the noise performance of Fe, Co, Si,

and B amorphous alloys in ring-core fluxgate magnetometers, Can. J. Phys., 63, 1468–1472, https://doi.org/10.1139/p85-246, 1985.

Nielsen, O. V., Petersen, J. R., Fernandez, A., Hernando, B., Spisak, P., Primdahl, F., and Moser, N.: Analysis of a fluxgate magnetometer based on metallic glass sensors, Meas. Sci. Technol., 2, 435–440, 1991.

Nielsen, O. V., Petersen, J. R., Primdahl, F., Brauer, P., Hernando, B., Fernandez, A., Merayo, J. M. G., and Ripka, P.: Development, construction and analysis of the 'OErsted' fluxgate magnetometer, Meas. Sci. Technol., 6, 1099–1115, 1995.

Nielsen, O. V., Afanassiev, Y., and Fornaçon, K. H.: Magnetic Materials for Sensors, in: Fluxgate Magnetometers for Space Research, edited by: Musmann, G., chap. 6, 152–168, 2010.

Nosenko, V. K., Maslov, V. V., Kirilchuk, V. V., and Kochkubey, A. P.: Some industrial applications of amorphous and nanocrystalline alloys, J. Phys. Conf. Ser., 98, 072016, https://doi.org/10.1088/1742-6596/98/7/072016, 2008.

Paperno, E.: Suppression of magnetic noise in the fundamental-mode orthogonal fluxgate, Sensor. Actuat. A-Phys., 116, 405–409, https://doi.org/10.1016/j.sna.2004.05.011, 2004.

Rax, B. G., Lee, C. I., and Johnston, A. H.: Degradation of precision reference devices in space environments, IEEE T. Nucl. Sci., 44, 1939–1944, https://doi.org/10.1109/23.658965, 1997.

Sasada, I. and Kashima, H.: Simple design for orthogonal fluxgate magnetometer in fundamental mode, Journal of the Magnetics Society of Japan, 33, 43–45, https://doi.org/10.3379/msjmag.0901RF7129, 2009.

Scandurra, G., Cannatà, G., Giusi, G., and Ciofi, C.: Programmable, very low noise current source, Review of Scientific Instruments, 85, 125109, https://doi.org/10.1063/1.4903355, 2014.

Shirae, K.: Noise in amorphous magnetic materials, IEEE T. Magn., 20, 1299–1301, https://doi.org/10.1109/TMAG.1984.1063504, 1984.

Texas Instruments Inc.: OPA2188 0.03-μV/°C Drift, Low-Noise, Rail-to-Rail Output, 36-V, Zero-Drift Operational Amplifiers, available at: http://www.ti.com/lit/ds/symlink/opa2188.pdf, 2016.

Tsividis, Y. P.: Accurate analysis of temperature effects in I_C–V_{BE} characteristics with application to bandgap reference sources, Solid-State Circuits, IEEE J. Solid-St. Circ., 15, 1076–1084, https://doi.org/10.1109/JSSC.1980.1051519, 1980.

Turbitt, C., Matzka, J., Rasson, J., St-Louis, B., and Stewart, D.: An instrument performance and data quality standard for intermagnet one-second data exchange, in: Proceedings of the XVth IAGA Workshop on Geomagnetic Observatory Instruments and Data Processing, Cadiz, Spain, 4–14 June 2012, edited by Hejda, P., Chulliat, A., and Catalán, M., 186–188, available at: http://nora.nerc.ac.uk/507228/1/Turbitt_etal_IAGAworkshop_OneSecondDataExchange_2013.pdf (last access: 2 July 2017), 2013.

Vetoshko, P., Valeiko, M., and Nikitin, P.: Epitaxial yttrium iron garnet film as an active medium of an even-harmonic magnetic field transducer, Sensor. Actuat. A-Phys., 106, 270–273, https://doi.org/10.1016/S0924-4247(03)00182-1, 2003.

Vishay Precision Group, Inc.: DSMZ (Z foil). Ultra High Precision Bulk Metal® Z-Foil Surface Mount Voltage Divider, TCR Tracking of < 0.1 ppm/°C, PCR of ± 5 ppm at Rated Power and Stability of ± 0.005 % (50 ppm), available at: http://www.vishaypg.com/docs/63121/dsmz.pdf (last access: 2 July 2017), 2015.

Vishay Precision Group, Inc.: VSMP Series (0603, 0805, 1206, 1506, 2010, 2512) (Z Foil) Ultra High Precision Foil Wraparound Surface Mount Chip Resistor, available at: http://www.vishaypg.com/docs/63060/VSMP.pdf (last access: 2 July 2017), 2016.